Constitution and Thermodynamics of Monotectic Alloys—A Survey

B. Predel
Max-Planck-Institut für Metallforschung
Institut für Werkstoffwissenschaft, Seestrasse 92, D-70174 Stuttgart, Germany
and University of Stuttgart, Institut für Metallkunde
Seestrasse 75, D-70174 Stuttgart

(Submitted 10 March 1997)

As is well known, melts that have passed a miscibility gap in the liquid state will, on cooling, solidify to a regulus consisting of two layers. Such bodies are not interesting for technical applications and have rarely been investigated. Genuine interest in demixing systems only arose once it seemed possible to prevent layer formation in zero gravity. However, experiments in space have shown that, even under micro-g conditions, phase separation occurs, though in a different way than on earth. This resulted in an intensive disclosure of the thermodynamics and the kinetics of the separation of liquid immiscible phases. After a discussion of the results obtained, the paper suggests how to prevent layer formation and how to effect a finely dispersed structure to enable technical use.

Introduction

In the past, systems that tend to form intermetallic phases had been of special interest. Of course, this is understandable if one is thinking of the possibilities of the technical application of these systems. On the other hand, alloys of systems that exhibit an extensive miscibility gap in the liquid state had no technical importance, at least about 40 years ago.

Figure 1 represents the Al-Pb phase diagram, as taken from the compilation of [58Han]. The miscibility gap in the liquid state

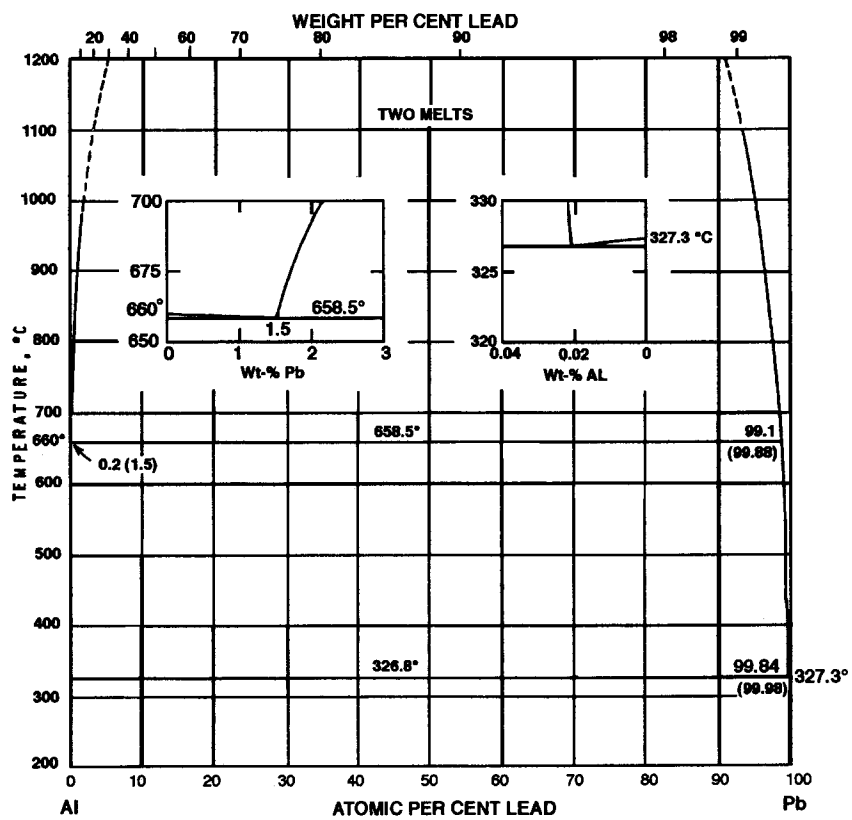

Fig. 1 Al-Pb phase diagram taken from [58Han].

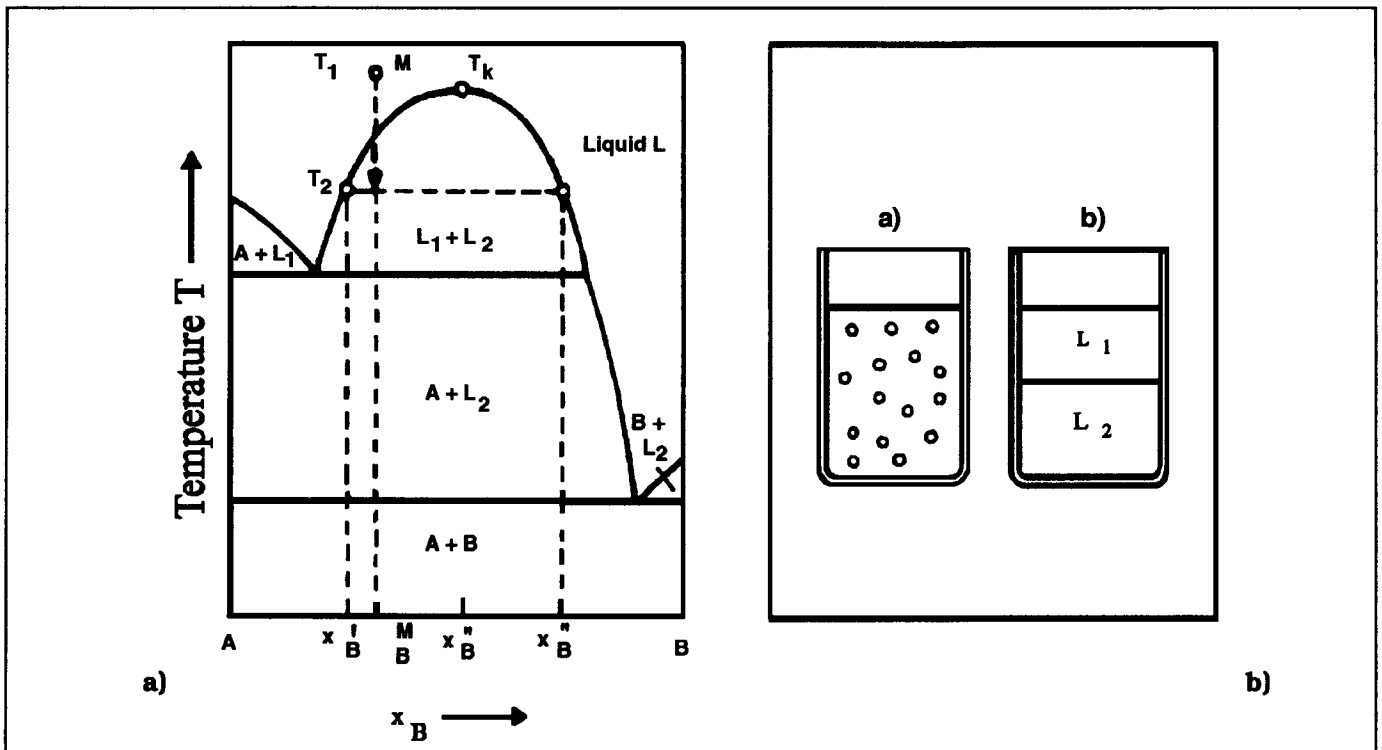

Fig. 2 Schematic representation of layer formation in a system with demixing tendency.

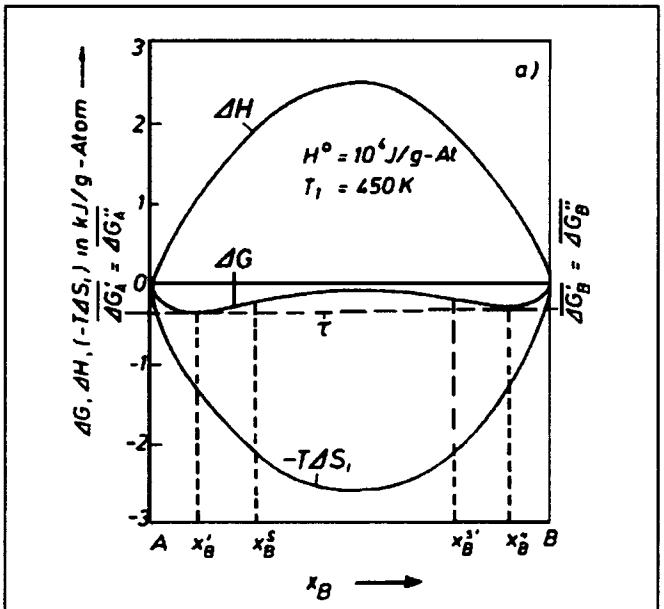

Fig. 3 Thermodynamic functions of a regular solution with $H^0 = 10^4$ J/g-atom at $T_1 = 450$ K.

is known only in the region of the monotectic temperature. An alloy that is single-phase at high temperatures passes the miscibility gap on cooling (see Fig. 2). During this process both liquid phases—due to their different densities—separate into two layers, one above the other. Subsequently, both melts solidify to a regulus, as schematically depicted in Fig. 2. Such a regulus has no value for technical applications.

Thermodynamics of Alloys with Demixing Tendency

With respect to their thermodynamics, systems with a miscibility gap have also been considered rather boring. To simplify, the regular solution model has been applied. According to that, for the enthalpy of mixing, there is:

$$\Delta_{mix}H = H^0 X_A(1 - X_A) \quad \text{(Eq 1)}$$

where X_A, $X_B = 1 - X_A$ are the mole fractions.

As is well known, the concentration dependence of the ideal entropy of mixing, ΔS_i as it is given for a random atomic distribution, is composed in the following way:

$$\Delta S_i = -R[X_A \ln X_A + X_B \ln X_B] \quad \text{(Eq 2)}$$

where H^0 is a constant containing the coordination number. R is the general gas constant.

Applying the regular solution model, the enthalpy of mixing has to be symmetrical, as is demonstrated in the example for $H^0 = 10^4$ J/g-atom in Fig. 3. The same is true for the ideal entropy of mixing. Accordingly, the miscibility gap has to be symmetrical (Fig. 4).

The simplifying treatment has changed somewhat during recent years.

There are indeed miscibility gaps that are nearly symmetrical, just as the regular solution model demands. An example is the following Hg-Ga phase diagram (Fig. 5).

The Bi-Ga and Bi-Zn systems ought to be mentioned as examples of asymmetrical miscibility gaps (Fig. 6, 7). This shape of miscibility gaps cannot be described by the simple regular solution model.

An important factor is the influence of the difference between the atomic radii of the components. In order to emphasize this influence, the critical demixing temperature T_c is considered. In Fig. 8, it is plotted as a function of the difference of the atomic radii. For simplification, systems were chosen in which one partner always remains the same to maintain constant possible bonding influences. Figure 8(a) represents such a plot for lead systems. With increasing difference of the radii, the critical demixing temperature T_c also increases. This is immediately connected with the maximal enthalpy of mixing $\Delta_{mix}H(L)$ which in Fig. 8(b) is plotted against the difference of the atomic radii. The bigger the atomic radii difference d, the bigger the positive maximum enthalpy of mixing. Therefore, the bigger the misfit energy, the smaller the mutual solubility of the components [66Pre, 80Pre].

The influence of the coordination number depending on radii differences is shown in Fig. 9. In this case, $X_{S,A}$ and $X_{S,B}$ are the fractions of atomic surface, which are taking part in the interatomic interaction. The quantities $X_{S,A}$ and $X_{S,B}$ have to be inserted, replacing X_A and X_B, respectively, in the regular solution model. The relationship between these quantities is given by:

$$X_{S,A} = \frac{X_A r_A^2}{X_A r_A^2 + X_B r_B^2}$$

$$X_{S,B} = \frac{X_B r_B^2}{X_A r_A^2 + X_B r_B^2} \qquad \text{(Eq 3)}$$

where r_A and r_B are the atomic radii.

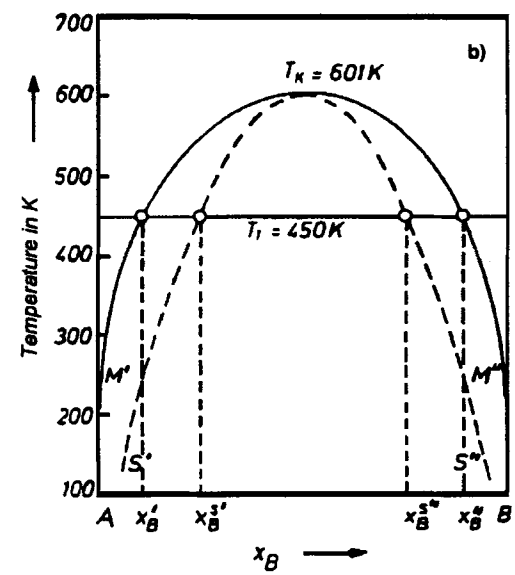

Fig. 4 Miscibility gap of a regular solution with energetic data of Fig. 3.

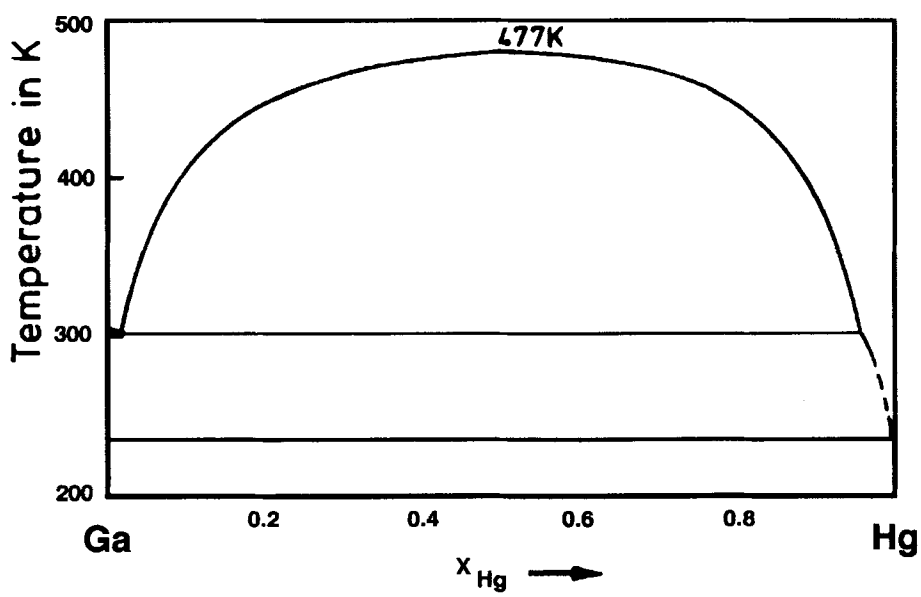

Fig. 5 Phase diagram of the Hg-Ga system [60Pre].

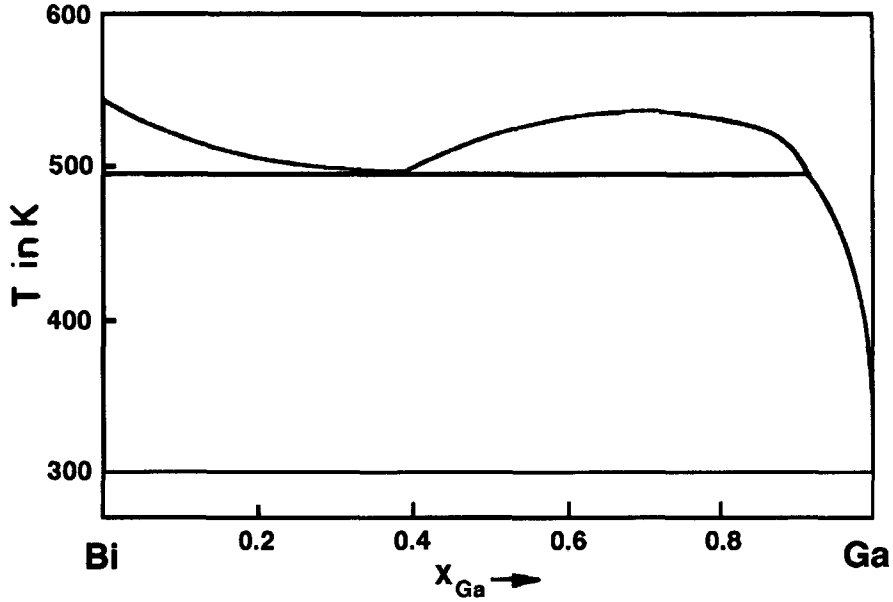

Fig. 6 Phase diagram of the Bi-Ga system [60Pre, 65Ell].

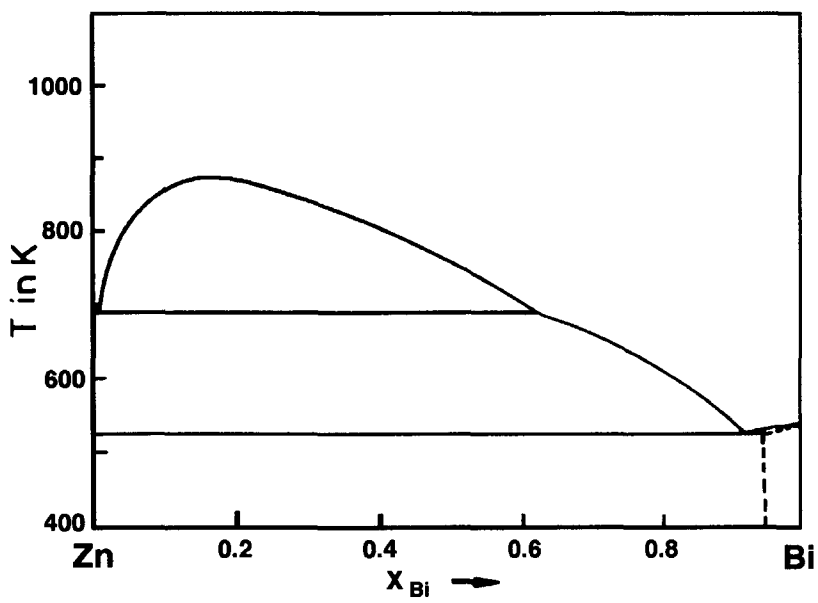

Fig. 7 Phase diagram of the Bi-Zn system [65Ell].

These considerations can be traced back to [62Lac] and [76Mie]. The enthalpy of mixing is now expressed by:

$$\Delta_{mix}H = C_{reg}X_{S,A}\,X_{S,B} \qquad \text{(Eq 4)}$$

To correctly express the entropy of mixing if there is a radii difference, [42Flo] and [42Hug] have modified Eq 2 (see [86Luc]). In this case, the molar fractions have to be replaced by the volume fractions:

$$X_{V,A} = \frac{X_A r_A^3}{X_A r_A^3 + X_B r_B^3}$$

$$X_{V,B} = \frac{X_B r_B^3}{X_A r_A^3 + X_B r_B^3} \qquad \text{(Eq 5)}$$

The entropy of mixing has to be written:

$$\Delta_{mix}S = -R(X_{V,A}\ln X_{V,A} + X_{V,B}\ln X_{V,B}) \qquad \text{(Eq 6)}$$

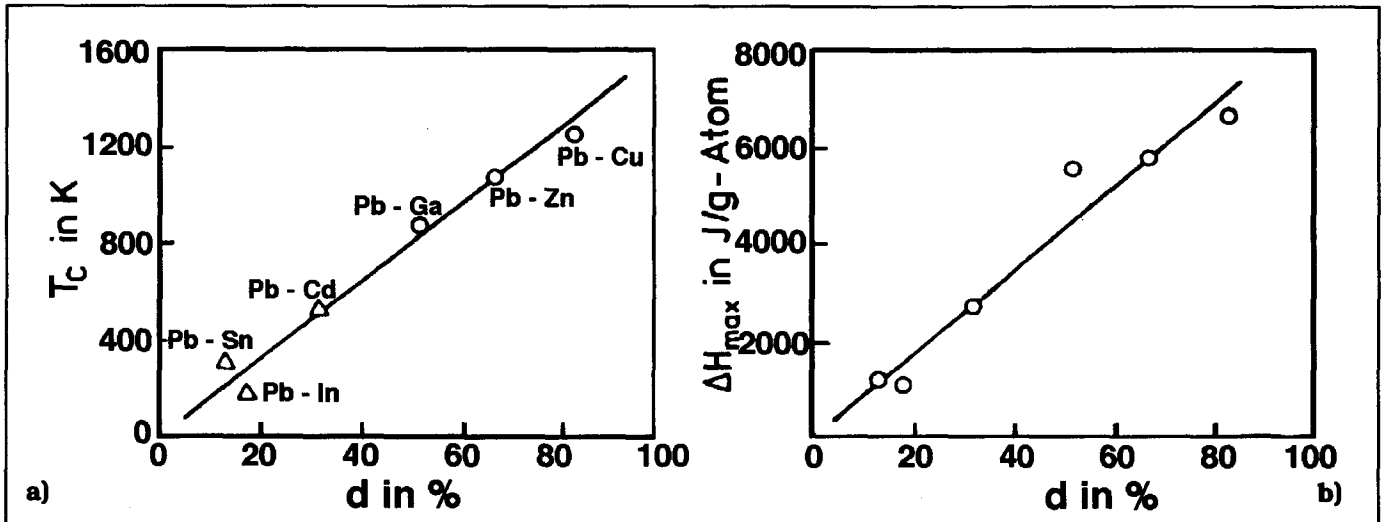

Fig. 8 T_C and ΔH_{max} as a function of atomic radii difference d. O, experimental; Δ, calculated [66Pre, 80Pre].

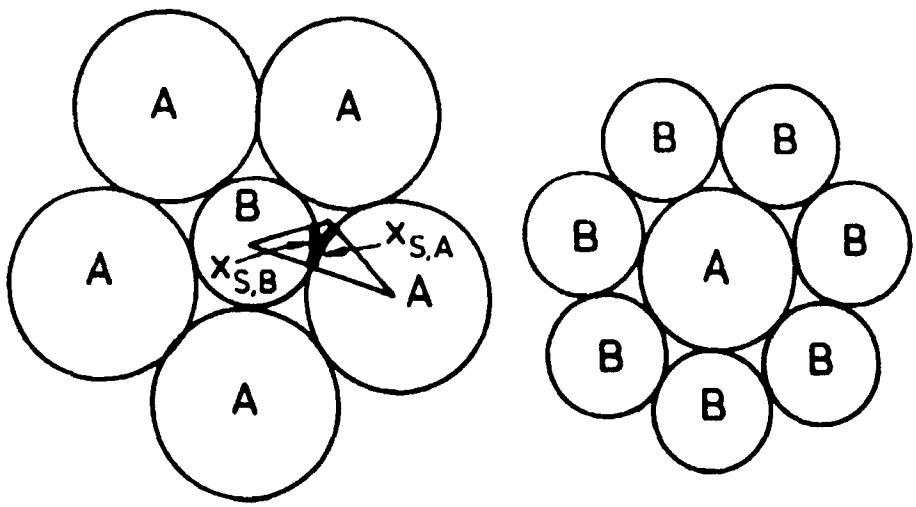

Fig. 9 Coordination number and atomic radii differences (see [87Pre]).

On the basis of the quasi-chemical approximation, [52Gug] and [62Mun] disclosed further terms for the Gibbs energy. The final relationship is:

$$\begin{aligned}\Delta G = {} & RT\left(X_{V,A}\ln X_{V,A} + X_{V,B}\ln X_{V,B}\right) + C_{reg}X_{S,A}X_{S,B} \\ & + \left[\frac{2RT}{Z} + C_{reg} - \frac{2RT}{Z}\exp\left(\frac{C_{reg}Z}{2RT}\right)\right]X_{S,A}^2X_{S,B}^2 \\ & + \left[\frac{6RT}{Z} + 2C_{reg} - \frac{8RT}{Z}\exp\left(\frac{C_{reg}Z}{2RT}\right)\right. \\ & \left. + \frac{2RT}{Z}\exp\left(\frac{C_{reg}Z}{RT}\right)\right]X_{S,A}^3X_{S,B}^3 \qquad \text{(Eq 7)}\end{aligned}$$

where Z is the coordination number. At high temperatures, all terms except the first two can be neglected.

The effect of the atomic radii difference is shown in Fig. 10 ($\Delta_{mix}H^0 = 10^4$ J/g-atom). Figure 10(a) represents $\Delta G - X$ curves at equality of the radii of the two kinds of atoms. Figure 10(b) shows the asymmetry for the case where $r_B/r_A = 1.33$. With increasing temperature, in Fig. 10(b) the $\Delta G - X$ curves become more similar. As already stated, with increasing temperatures the influence of the higher terms (from the third term upward) decreases more and more.

Miscibility Gaps in Systems with Strong Tendencies toward Compound Formation

An example is the Ag-Te system [82Som]. Figure 11 shows the phase diagram for $X_{Te} < 0.4$. In addition to an intermetallic

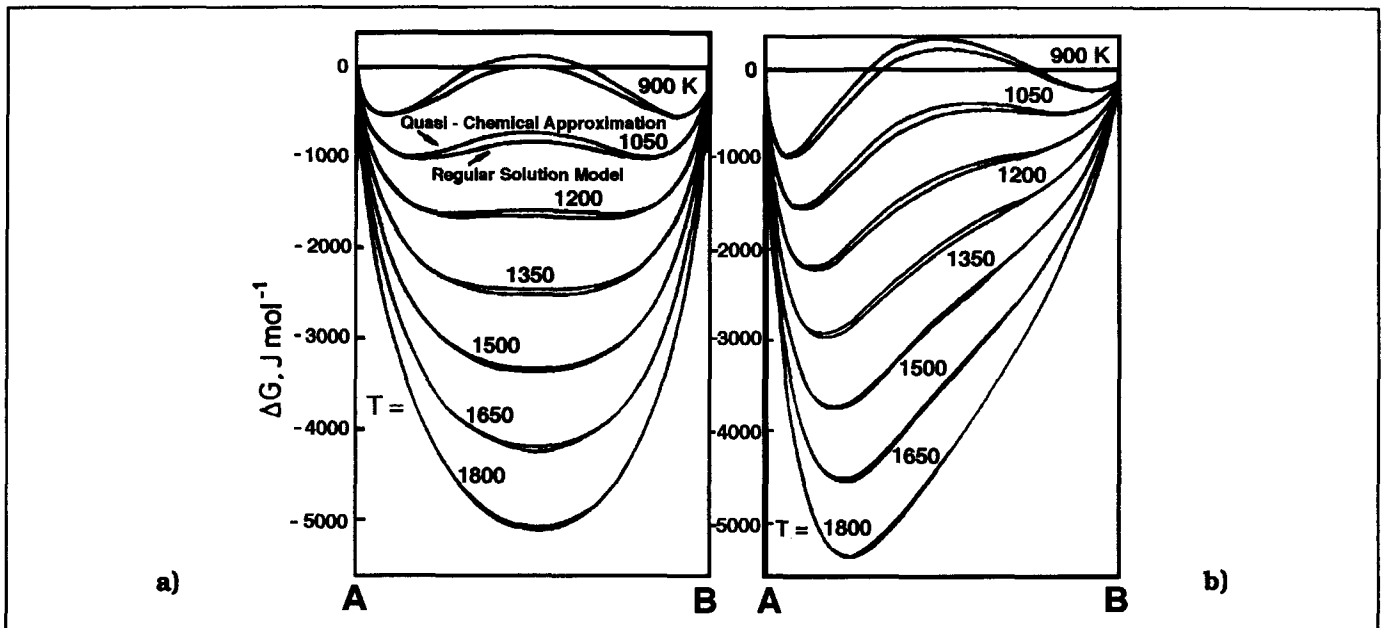

Fig. 10 Gibbs enthalpies of mixing (see [87Pre]). **(a)** For systems with equal atomic radii. **(b)** For a system with $r_A/r_B = 1.33$.

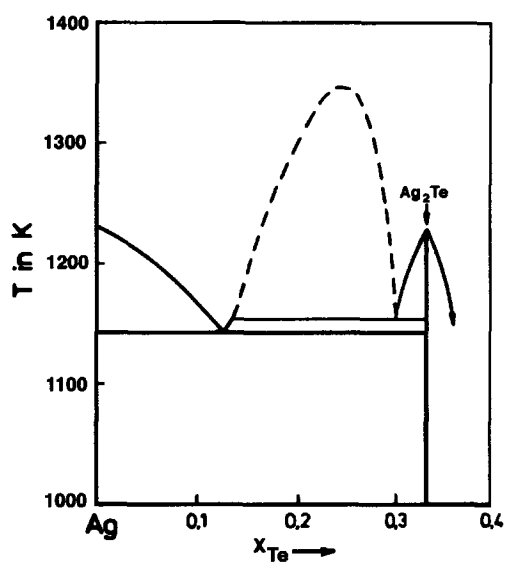

Fig. 11 Partial phase diagram of the Ag-Te system [82Som].

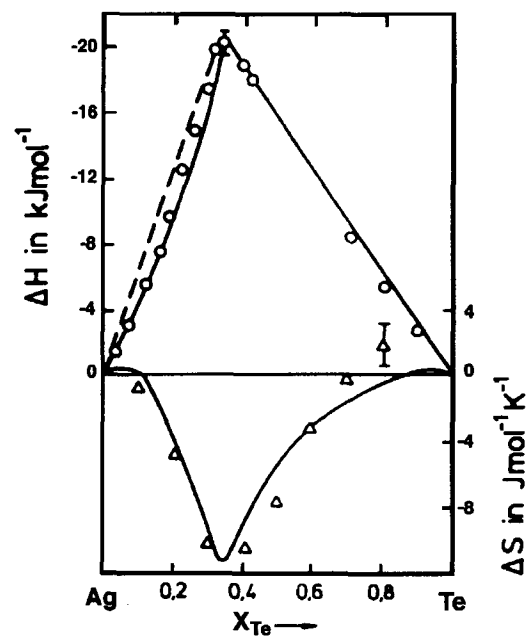

Fig. 12 Thermodynamic functions of the Ag-Te system [82Som].

phase Ag_2Te, a miscibility gap occurs in the liquid state. Here, the atomic structure of the melt plays an important role.

In addition to the monoatomic species Ag and Te, moleculelike associations Ag_2Te are present in the melt. Generally, in such cases there is:

$$iA_1 + jB_1 \leftrightarrow A_iB_j \qquad \text{(Eq 8)}$$

where i and j are the stoichiometric coefficients of the associations.

For the total number of moles, there is:

$$n = n_{A_1} + n_{B_1} + n_{A_iB_j} \qquad \text{(Eq 9)}$$

Here, n_{A_1}, n_{B_1}, and $n_{A_iB_j}$ are the numbers of moles of A_1, B_1, and A_iB_j, respectively.

The association equilibrium must be in accordance with the mass action law:

$$\frac{X^i_{A_1} X^j_{B_1}}{X_{A_iB_j}} = \frac{1}{K_{A_iB_j}} \qquad \text{(Eq 10)}$$

For the concentration dependence of the enthalpy of mixing results:

$$\Delta_{mix}H = H^0_{A_1B_1}\frac{n_{A_1}n_{B_1}}{n} + H^0_{A_1,A_iB_j}\frac{n_{A_1}n_{A_iB_j}}{n} + H^0_{B_1,A_iB_j}\frac{n_{B_1}n_{A_iB_j}}{n} + n_{A_iB_j}\Delta H^0_{A_iB_j} \qquad \text{(Eq 11)}$$

where $H^0_{A_1,B_1}$, $H^0_{A_1,A_iB_j}$, and $\Delta H^0_{B_1,A_iB_j}$ are the constants of the interaction between the species characterized by indexes. In the case of the presence of an association equilibrium, the concentration dependence of the entropy of mixing may be given by:

$$\Delta S = -R\left(n_{A_1}\ln X_{A_1} + n_{B_1}\ln X_{B_1} + n_{A_iB_j}\ln X_{A_iB_j}\right) + n_{A_iB_j}\Delta S^0_{A_iB_j} \qquad \text{(Eq 12)}$$

where $\Delta S^0_{A_iB_j}$ is the molar entropy of formation of the associates.

The ΔH-X curve has a triangular shape, with its apex at the stoichiometry of the associations (Ag_2Te, see Fig. 12). The ΔH values between 0 and 33 at.% Te deviate from the straight line plotted in the figure to lower negative values. This is due to an interaction between the associations and the Ag atoms in the melt (second term in Eq 11). This indicates a demixing tendency in this concentration range. Results of thermodynamic calculations carried out by [82Som] indeed show a miscibility gap in the liquid state in this region (see Fig. 11).

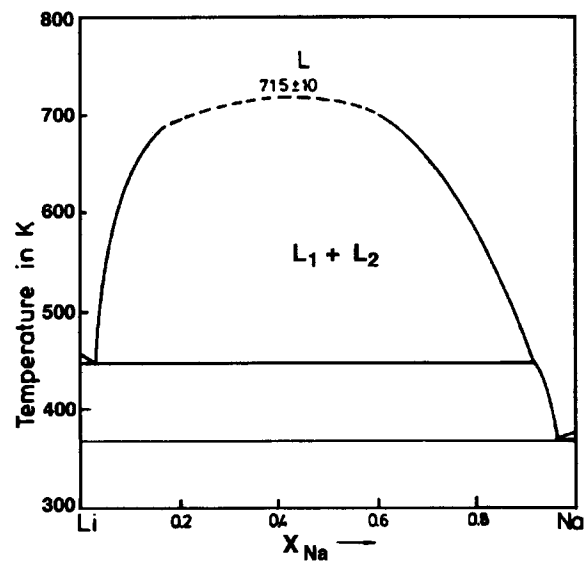

Fig. 13 Miscibility gap in the Li-Na system (from [65Ell]).

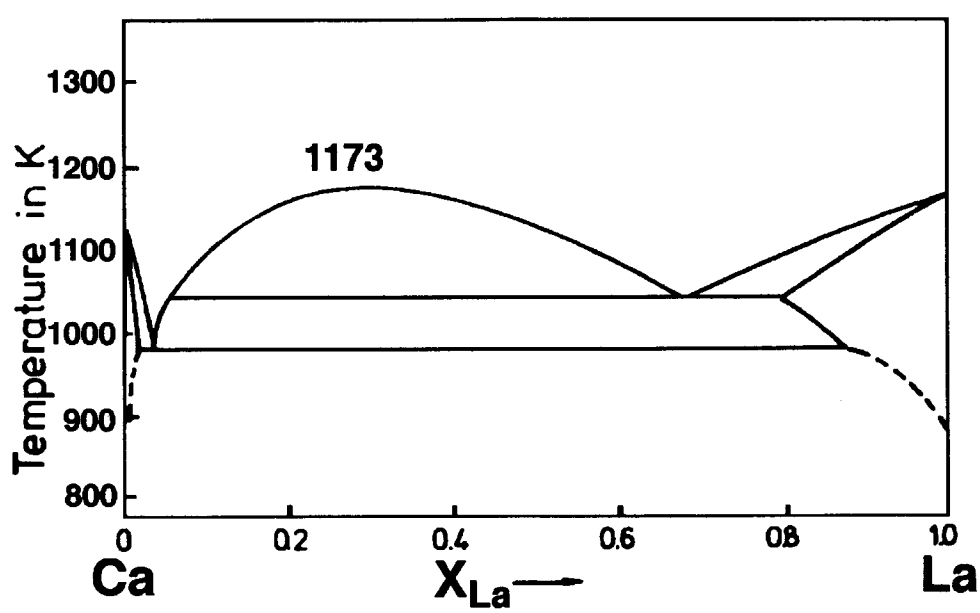

Fig. 14 Miscibility gap in the Ca-La system (see [65Ell]).

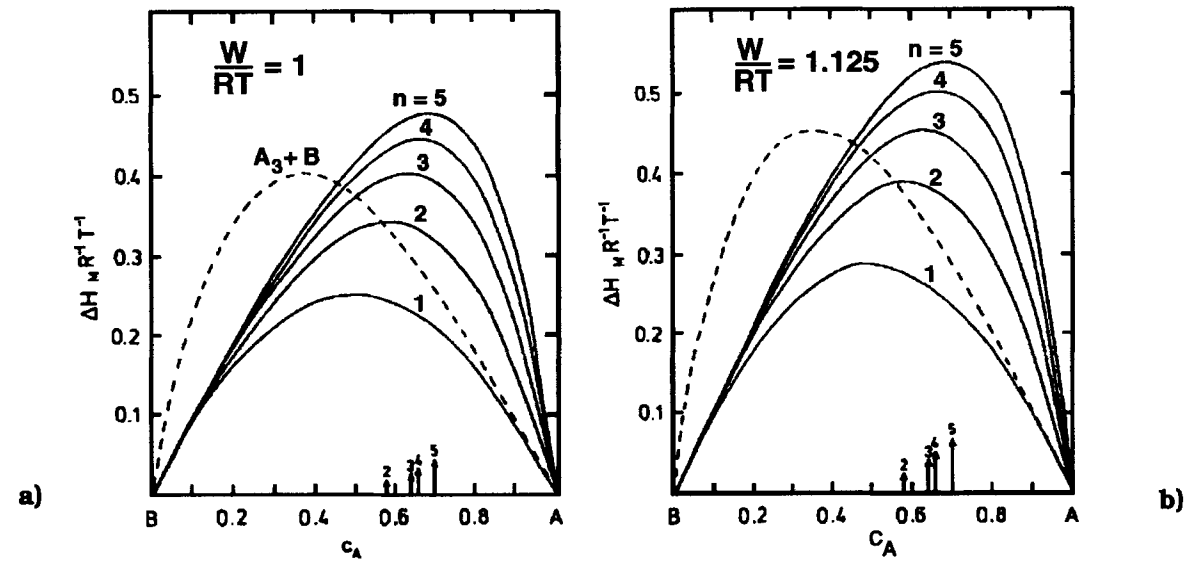

Fig. 15 Enthalpy of mixing calculated for different values of n and W/RT, assuming self-associations of the type B_n and A_3 (taken from [92Sin]).

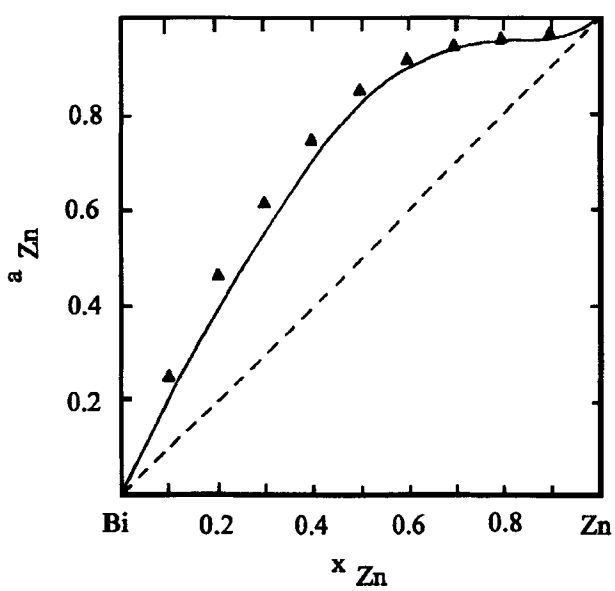

Fig. 16 Thermodynamic activities of Zn in liquid Bi-Zn alloys at $T = 900$ K calculated using the association model. Δ, [93Wan] optimizing calculations.

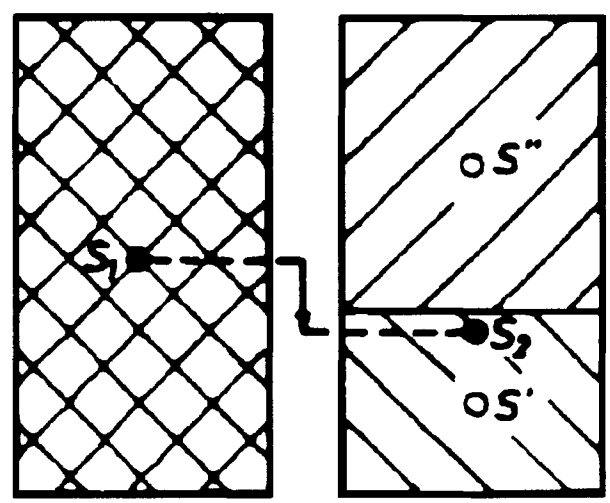

Fig. 17 Schematic representation of gain of potential energy on layer formation. S_1, center of gravity of homogeneous sample; S', center of gravity of the lower layer; S'', center of gravity of the upper layer; S_2, center of gravity of the demixed sample.

Further Examples of the Occurrence of Miscibility Gaps in the Liquid State

As mentioned before, miscibility gaps in the liquid state can also occur in systems with compound formation tendency. But, in most cases, they are typical in systems that have a rather high value of positive $\Delta_{mix}H(L)$. This positive $\Delta_{mix}H(L)$ value can result from different features. Some more examples are mentioned.

Miscibility gaps in the liquid state occur in some systems that are composed of a transition metal and a main group element. An example is the Ni-Pb system. For many such systems, the shape of the miscibility gap is not yet known.

Also, if no strong influence of the bonding conditions is expected, the atomic radii difference can be solely responsible for the miscibility gap (shown in Fig. 8 for some combinations of main group elements). Included in this group of binary sys-

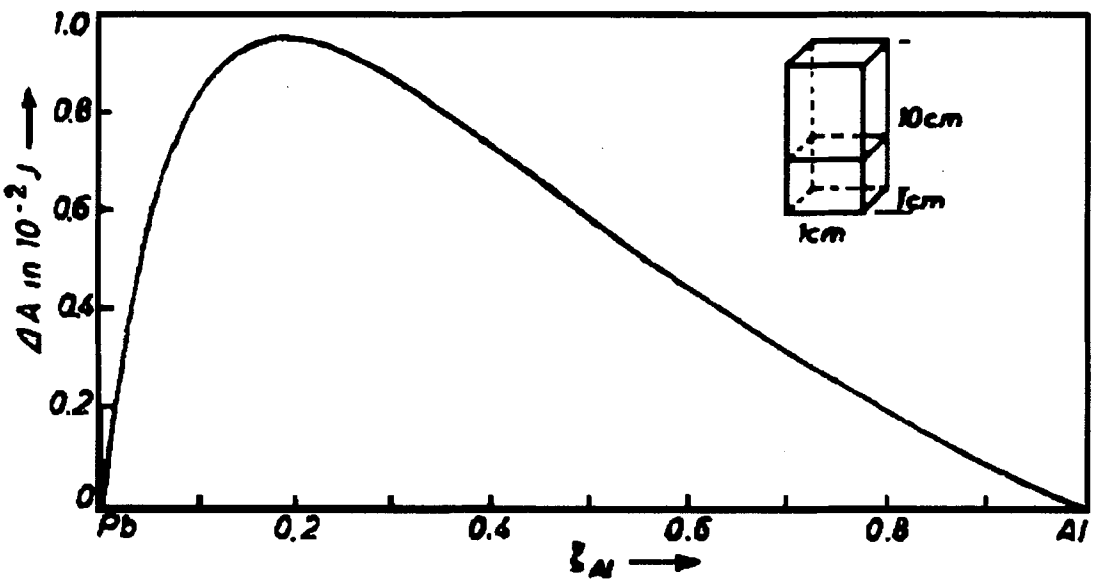

Fig. 18 Gain of potential energy ΔA as a function of mass fraction ζ_{Al} on layer formation in the Al-Pb system (see [80Pre]).

tems are also combinations of elements of the same group, as seen in Fig. 13 for the Li-Na system.

However, if no essential atomic radii difference is present, as in the Ca-La system, the difference of the valences of the components can result in a positive $\Delta_{mix}H(L)$ and, accordingly, to a miscibility gap in the liquid state (see Fig. 14).

Even in binary systems in which neither an appreciable atomic radii difference is present nor significant bonding effects are expected—as in systems of two rare earth metals—a miscibility gap can be found, for example, in the Eu-Sc and Yb-Tb systems, in which the electronic configurations of the partners are different.

The association model can help to describe rather well the thermodynamic properties of liquid alloys with compound formation tendencies. It suggests itself as a way to develop an analogous model also for systems with demixing tendencies. For that purpose, [92Sin] have developed the following conceptions.

First, the occurrence is assumed to have clusters of the same kinds of atoms, namely Ai and Bj, where i and j are the numbers of atoms in the respective clusters. Fundamental to further consideration is the quasi-lattice statistical mechanical theory proposed by [84Bha]. According to this model, the asymmetry of $\Delta_{mix}H$ and $\Delta_{mix}S^{ex}$ should be expected if the number i of atoms in the clusters A, and the number j of atoms in the clusters B, are not equal. The amount of $\Delta_{mix}H$ is bigger in the A-rich concentration region than in the B-rich alloys, if $j > i$. Also, the maximum amount of $\Delta_{mix}H$ is dependent on $j/i = n$. This is shown in Fig. 15 for $W/(RT) = 1$. Here, there is:

$$\Delta_{mix}H = X_A X_B \eta W - X_A X_B \eta T \frac{dW}{dT} + RT^2 X_A X_B \eta \left(\frac{\beta}{1-\beta} - X_A \eta \frac{W}{RT} \right) \frac{\partial \beta}{\partial T} \qquad \text{(Eq 13)}$$

with

$$\beta = 1 - \frac{1}{\eta}, \eta = \frac{1}{1 - \beta X_A},$$

$$W = i\omega,$$

and

$$\omega = z\left(\varepsilon_{AB} - \frac{\varepsilon_{AA}}{2} - \frac{\varepsilon_{BB}}{2} \right)$$

where ω is the interaction energy. The larger η is, the greater are both the asymmetry and the amount of the maximum enthalpy of mixing.

The entropy of mixing, too, is changed by the formation of self-associations. As an example of the usefulness of these model conceptions, Fig. 16 presents an activity isotherm of Zn in the Bi-Zn system for 900 K. The points drawn in the plot comply with the results of an optimizing calculation [93Wan]; the line drawn through represents the activity isotherm calculated by [92Sin] using the model already indicated.

Energetics of Layer Formation in the Gravity Field of Earth

On passing through a miscibility gap, at first a finely dispersed precipitation occurs (see Fig. 2). In the gravity field of earth, the tiny droplets are rapidly transformed into layers, one above the other. The kinetics of this process consist of diffusion, convection, and movement by buoyancy caused by density differences. The lowering of the center of gravity caused by these processes results in a potential energy gain, as can be seen in Fig. 16. Of course, this potential energy gain is dependent on the concentration. For the case of the Al-Pb system, this can be seen from Fig. 17. There, the potential energy gain ΔA is plotted against the mass fraction:

$$\zeta_{Al} = \frac{m_{Al}}{m_{Al} + m_{Pb}} \qquad \text{(Eq 14)}$$

The shape of the sample assumed is shown in the partial Fig. 18. In this case, m_{Al} and m_{Pb} are the masses of the Al-rich and Pb-rich layers, respectively.

The maximum of ΔA lies, under the said limiting conditions, at about $\Delta A = 1 \times 10^{-2}$ J. This value is observed at $\zeta_{Al} = 0.2$, which complies with approximately 66 at.% Al (see [80Pre]).

It should be noted that, until the monotectic temperature is reached, at this concentration and on the basis of the thermodynamic data on demixing reported by [73Hul], ΔG is lowered by 4.3 kJ/g-atom. Layer formation in the gravitational field of earth results in a relatively small decrease of the Gibbs energy of the total system.

The decrease of the potential energy, however, is sufficient to cause, in a sample of 10 cm height, complete phase separation within less than 10 s. This is obviously due to the low viscosity in liquid Pb-Al alloys. An estimation regarding the cooling rate, which must be applied to prevent layer formation, leads to values ranging from 10^6 to 10^{10} K/s. This is on an order of magnitude that can be reached by splat cooling. In doing so, no compact samples can be obtained, but only very thin foils.

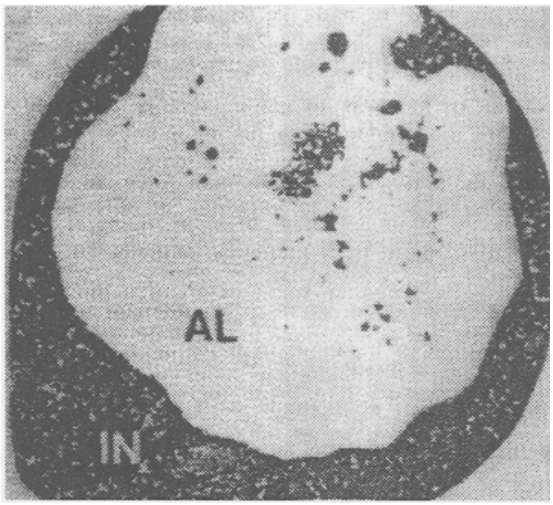

Fig. 19 Al-In alloy in the result of a rocket experiment [79Ahl].

Demixing under Micro-g Conditions

There was hope of obtaining finely dispersed materials in demixing systems under space conditions. In doing so, sam-

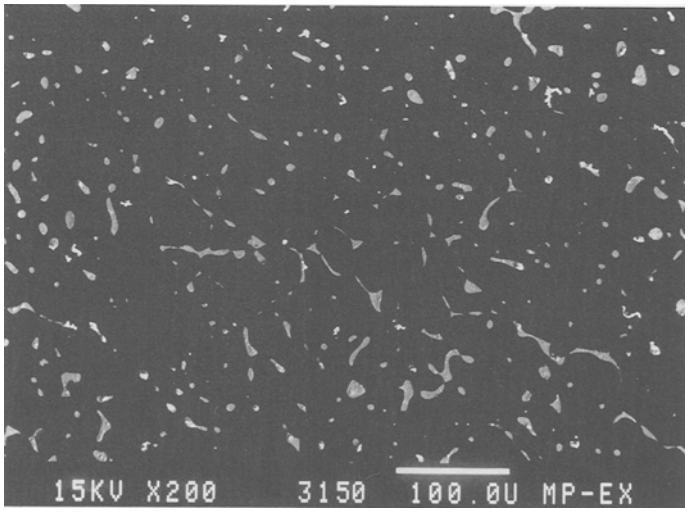

Fig. 20 Microstructure of an Al-10%Pb-10%Sn-3%Cu composite prepared with ultrasonic power [95Abr2]. Black, aluminium matrix; white, fine inclusions, which are rich in Pb with additional up to 12 wt.% Sn.

ples were cooled down from the region above the miscibility gap until they were entirely solidified (Apollo 14 and 16, Skylab). The result, as it has been achieved by [80Reg] in 1980 in the Pb-Zn system, was disappointing. It was not possible to establish that there are any differences between samples that had solidified on earth and samples that had been cooled down under micro-g conditions. Later, space experiments were carried out by [79Ahl] with Al-In alloys in Al_2O_3 crucibles. These investigations have shown interesting successes. Figure 19 reproduces a metallographic section of a sample solidified in space. The In-rich liquid phase has assembled at the periphery of the sample. Certainly, on the separation of the two molten volume parts the reduction of the entire surface energy is of crucial importance.

Applications

As stated at the beginning, a regulus consisting of two layers is useless for technical applications. In addition, solidification under micro-g conditions does not yield finely dispersed solid materials. A finely dispersed distribution of both phases, however, would result in an increase of strength, as the gliding of dislocations is inhibited. In this process, particle size and the volume fraction are of special importance.

Monotectic alloys with finely dispersed distribution in a solid phase probably have high wear resistance. This would make them usable for electrical switch contacts.

Finally, self-lubricating bearings could be constructed from finely dispersed alloys. The matrix would probably be mechanically strong, and the dispersed phase relatively soft. If the dispersed phase consists of indium or lead, excellent properties can be expected. Fine, abraded particles could be accepted by the friction bearing, thus protecting the bearing against rapid wear.

Production of Finely Dispersed Demixing Alloys on Earth

There have been repeated attempts to attain, also under 1 g conditions, a finely dispersed distribution of the phases on passing through a miscibility gap. In particular, the works of [95Abr1] should be mentioned. These authors compensate for the gravity field of the earth, which leads toward layer formation by a Lorentz force. At the same time, an ultrasonic vibration is generated to prevent coagulation. The micrograph of an Al-10%Pb-10%Sn-3%Cu (all wt.%) alloy treated in this way is reproduced in Fig. 20 [95Abr2].

Obviously it is possible, by the abovementioned magnetic and electric cross-fields as well as by ultrasonic vibration, to produce a homogeneous distribution of dispersed Pb-rich phase in an Al-base matrix alloy.

Cited References

42Flo: P.J. Flory, *J. Chem. Phys., 10,* 51 (1942).

42Hug: M.L. Huggins, *J. Phys. Chem., 46,* 151 (1942).

52Gug: E.A. Guggenheim, *Mixtures,* Oxford (1952).

58Han: M. Hansen and K. Anderko, *Constitution of Binary Alloys,* McGraw-Hill, New York (1958).

60Pre: B. Predel, *Z. Phys. Chem., 24,* 206 (1960).

62Lac: R. Lacman, *Z. Phys. Chem., Neue Folge, 35,* 86 (1962).

62Mun: A. Münster, "Statistische Thermodynamik Kondensierter Phasen," *Handbuch der Physik,* S. Flügge, Ed., Springer, Berlin (1962).

65Ell: R.P. Elliott, *Constitution of Binary Alloys, First Supplement,* McGraw-Hill, New York (1965).

66Pre: B. Predel, *Acta Metall., 14,* 209 (1966).

73Hul: R. Hultgren, P.D. Desai, D.T. Hawkins, M. Gleiser, and K.K. Kelley, *Selected Values of Thermodynamic Properties of Binary Alloys,* American Society for Metals, Metals Park, OH (1973).

76Mie: A.R. Miedema, *J. Less-Common Met., 46,* 67 (1976).

79Ahl: H. Ahlborn and K. Löhberg, "Aluminium-Indium Experiment—A Sounding Rocket Experiment on Immiscible Alloys," paper 79-0172, 17th AJAA Conf. New Orleans (1979).

80Pre: B. Predel and I. Arpshofen, *Metall, 34,* 412 (1980).

80Reg: J.L. Reger, *Material Processing in Space: Early Experiments,* NASA, Washington, D.C. (1980).

82Som: F. Sommer, *Z. Metallkde., 73,* 72, 77 (1982).

84Bha: A.B. Bhatia and R.N. Singh, *Phys. Chem. Liq., 13,* 177 (1984).

86Luc: R. Lück, U. Gerling, and B. Predel, *Z. Metallkde., 77,* 140 (1986).

87Pre: B. Predel, L. Ratke, and H. Fredriksson, "Systems with a Miscibility Gap in the Liquid State," *Fluid Science and Materials Science in Space,* Springer Verlag, Berlin (1987).

92Sin: R.N. Singh and F. Sommer, *Z. Metallkde., 83,* 7 (1992).

93Wan: Z.C. Wang, S.K. Yu, and F. Sommer, *J. Chem. Phys., 90,* 379 (1993).

95Abr1: V.O. Abramov, O.V. Abramov, F. Sommer, and D. Orlov, *Mater. Lett., 23,* 17 (1995).

95Abr2: V.O. Abramov, O.V. Abramov, F. Sommer, and D. Orlov, *Proc. Ultrasonic World Congress 1995,* J. Herberts, Ed., GEFAU, University of Duisburg, Germany, 729 (1995).